Flow force and torque on submerged bodies in lattice-Boltzmann via momentum exchange

Juan P. Giovacchini[1,3*] and Omar E. Ortiz[2,3†]
[1] *Departamento de Mecánica Aeronáutica, Instituto Universitario Aeronáutico, Córdoba, Argentina.*
[2] *Facultad de Matemática, Astronomía y Física, Universidad Nacional de Córdoba, Argentina.*
[3] *Instituto de Física Enrique Gaviola (CONICET), Córdoba, Argentina.*

We review the momentum exchange method to compute the flow force and torque on a submerged body in lattice Boltzmann methods by presenting a new derivation. Our derivation does not depend on a particular implementation of the boundary conditions at the body surface and relies on general principles. After the introduction of momentum exchange method in lattice Boltzmann some new formulations were introduced to compute the fluid force on static and moving bodies. These formulations were introduced in a rather intuitive, ad-hoc way. In our derivation we recover the proposals most frequently used, in some cases with minor corrections, gaining some insight into the two most used formulations. At the end we present some numerical tests to compare different approaches on well know benchmark test that support the correctness of the formulas derived.

PACS numbers: 47.11.-j, 47.10.-g, 51.10.+y

I. INTRODUCTION

During the last twenty-five years the Lattice-Boltzmann methods (*LBM*) have been greatly developed in many aspects. Today they can be used, to treat multiple problems involving both compressible and incompressible flows on simple and complex geometrical settings. For a complete modern review of this topic see [1].

It is of crucial importance, in many applications that involve moving bodies surrounded by a fluid flow, to have a good method or algorithm to compute the flow force and torque acting on the bodies. By good we mean a method that is simple to apply, that is accurate and fast, so as not to spoil the efficiency of the flow computing method. For a review of LBM methods that involve flow force evaluation on suspended particles we refer to Section 6 of [1] and references therein. We mention below some particular aspects of this subject that are of interest for the present article.

The classical way to compute forces, and so torque, on submerged bodies is via the computation and integration of the stress tensor on the surface of the body. In LBM the stress tensor is a local variable, its computation and extrapolation from the lattice to the surface is computationally expensive, which ruins the efficiency of the LBM. However, this method is widely used in LBM [2–4].

In 1994 Ladd introduced the *momentum exchange* (*ME*) in LBM to compute the flow force on a submerged body [5, 6]. Ladd's idea was rather heuristic and very successful, where the force is obtained by accounting the exchange of momentum between the surface of the body and the fluid, the latter being represented by "fluid particles" whose momentum is easily written in terms of the LBM variables that describe the fluid at the mesoscopic scale. Aidun et. al. [7, 8] introduce some improvements to Ladd proposal, obtaining a robust method to analyze suspended solid particles, and excluding the simulation of the interior fluid with a modified midway bounce-back boundary condition. Then, using boundary condition method to arbitrary geometries, Mei et. al. [9] proposed a method to evaluate the fluid forces from the idea of ME.

The ME algorithm is specifically designed and adapted to LBM; it is therefore more efficient than stress integration from the computational point of view.

The ME algorithm has been tested and applied successfully to a variety of problems [6, 9, 10]. For the mentioned ME methods, except the presented in [8], some accuracy problems have been detected though, when applied to moving bodies [4, 11].

Some approaches to improve the methods in problems with moving bodies were made. Wen et. al. [11], based in the proposal of [8] gives corrections terms to the forces given from [9]. Others alternative improved ME methods, based in the evaluation of force respect to a moving frame of reference, were proposed in [12].

The main goal of this paper is to provide a formal derivation of the momentum exchange algorithm. This new derivation provides insight and small corrections to some ad-hoc modifications proposed by Mei et. al. [9] and also to some newer, improved versions of momentum exchange algorithm presented in [11, 12].

The rest of the paper is organized as follows. In section II we briefly discuss the lattice-Boltzmann method with the main purpose of introducing notation; the method used to treat boundary conditions is also explained in this section. In Section III, the core of the paper, we present a derivation of the momentum exchange method to determine both, the flow force and torque on static or moving bodies. In section IV we present two numerical tests where we implement the methods derived in section III. In section V we make some comments.

*Electronic address: giovacchini@famaf.unc.edu.ar
†Electronic address: ortiz@famaf.unc.edu.ar

II. THE LATTICE-BOLTZMANN METHOD

In this section we present the basic equations of the lattice Boltzmann methods with the main purpose of introducing the notation used along the paper. For a thorough description of the Boltzmann equation we refer to [13, 14]. For a more complete presentation of LBM we refer to [15–17].

The Boltzmann equation (*BE*) governs the time evolution of the single-particle distribution function $f(\mathbf{x}, \boldsymbol{\xi}, t)$, where $\mathbf{x}$ and $\boldsymbol{\xi}$ are the position and velocity in phase space. The lattice Boltzmann equation (*LBE*) is a discretized version of the Boltzmann equation, where $\mathbf{x}$ takes values on a uniform grid (the lattice), and $\boldsymbol{\xi}$ is not only discretized, but also restricted small number of values [18]. By far the models used most frequently are the ones with collision integral simplified according to the Bhatnagar, Gross, and Krook (*BGK*) approximation [19] with relaxation time τ. In an isothermal situation and in the absence of external forces, like gravity, the LBE of this models read

$$f_i(\mathbf{x}_A + \mathbf{c}_i\delta t, t+\delta t) = f_i(\mathbf{x}_A, t) - \frac{1}{\tau}\Big(f_i(\mathbf{x}_A, t) - f_i^{eq}(\mathbf{x}_A, \rho, \mathbf{u}, t)\Big), \quad i = 0, 1, \ldots, Q-1. \quad (1)$$

Here $f_i = \omega_i f(\mathbf{x}_A, \mathbf{c}_i, t)$ is the i-th component of the discretized distribution function at the lattice site x_A, time t, and corresponding to the discrete velocity $\mathbf{c}_i$. ω_i is the i-th quadrature weight (explained below), and Q the number of discrete velocities in the model. In compressible-flow models the lattice constant δx, that separate two nearest neighbor nodes, and the time step δt are related with the speed of sound $c/\sqrt{3}$ by $\delta x = c\delta t$ [30]. The coordinates of a lattice node are $\mathbf{x}_A$, where the integer multi index $A = (j, k, l)$ (or, $A = (j, k)$ in the two-dimensional case) denotes a particular site in the lattice. The equilibrium distribution function f^{eq} is a truncated Taylor expansion of the Maxwell-Boltzmann distribution.

The macroscopic quantities such as the fluid mass density $\rho(\mathbf{x}, t)$, and velocity $\mathbf{u}(\mathbf{x}, t)$, are obtained, in Boltzmann theory, as marginal distributions of f and $\boldsymbol{\xi} f$ when integrating over $\boldsymbol{\xi}$. In LBM this integrals are approximated by proper quadratures. Specific values of c_i's and ω_i's, $i = 0, 1, \ldots, Q-1$, are made so that these quadratures give exact results for the $\boldsymbol{\xi}$-moments of order 0, 1 and 2 [17, 18]. We have

$$\rho(\mathbf{x}_A, t) = \sum_{i=0}^{Q-1} f_i(\mathbf{x}_A, t), \quad (2)$$

and

$$\rho\mathbf{u}(\mathbf{x}_A, t) = \sum_{i=0}^{Q-1} \mathbf{c}_i f_i(\mathbf{x}_A, t). \quad (3)$$

In the simulations we present in this paper, we are interested in incompressible flow problems, where we modify Eq. 3 according to the quasi-incompressible approximation presented in [20]. In this approximation ρ is replaced by ρ_0, a constant fluid mass density.

A single time step of the discrete evolution equation (1) is frequently written as a two-stage process

$$\hat{f}_i(\mathbf{x}_A, t) = f_i(\mathbf{x}_A, t) - \frac{1}{\tau}\Big(f_i(\mathbf{x}_A, t) - f_i^{eq}(\mathbf{x}_A, \rho, \mathbf{u}, t)\Big), \quad (4)$$

and

$$f_i(\mathbf{x}_A + \mathbf{c}_i\delta t, t+\delta t) = \hat{f}_i(\mathbf{x}_A, t). \quad (5)$$

The computation of $\hat{f}_i$ on the whole lattice, Eq. (4), is called the *collision step*, while the computation of f_i at $t + \delta t$, Eq. (5), on the whole lattice is called *streaming step.*

A. Treatment of boundary conditions

Many methods have been proposed in the literature to implement boundary conditions on moving boundaries with complex geometries in LBM. The method introduced in [21], later improved in [22, 23], has been extensively tested and is the one we use in the simulations presented in this paper[31]. We explain this method briefly in what follows. We emphasize that our derivation of momentum exchange is completely independent of the boundary condition method selected to perform the numerical tests.

We consider a body that fills a region Ω with closed boundary $\partial\Omega$ immersed in a fluid flow, and concentrate in a small portion of the boundary and its surrounding fluid as shown in Figure 1. The lattice nodes and links are also shown in the figure. Empty circles represent nodes lying inside the body region (solid nodes), while filled circles and squares represent nodes lying in the fluid region at the time shown. At time t a piece of boundary lie, in general, between lattice nodes. Consider a node F on the fluid with a neighbor node A inside the body. To determine the values of $f_i(\mathbf{x}_F = \mathbf{x}_A + \mathbf{c}_i\delta t, t+\delta t)$, the streaming step needs "non-existent" information coming from node A. It is the LBM implementation of the boundary conditions what provides this information with the desired accuracy.

The implementation of boundary conditions in LBM can be thought, at mesoscopic scale, as the introduction of a fluid flow inside Ω. It is this artificial flow what provides the needed information to evolve the outer flow so that it satisfies the right macroscopic boundary conditions at $\partial\Omega$. Even when the boundary $\partial\Omega$ is a physical boundary for the fluid, the mesoscopic LBM description of the fluid allow the fluid "particles" to stream across the surface $\partial\Omega$, both from inside out and viceversa.

We present here some particular proposals that will be used in section IV. From now on we refer as "boundary nodes" those lattice nodes on the fluid side, like F, that are involved in the imposition of boundary conditions.

The method presented in [21] proposes to determine $\hat{f}_i(\mathbf{x}_A, t)$ so that the linearly interpolated velocity at the boundary point B is the correct boundary velocity at that point. This is

$$\hat{f}_i(\mathbf{x}_A, t) = (1-\chi)\hat{f}_{\bar{i}}(\mathbf{x}_A + \mathbf{c}_i\delta t) + \chi g_{\bar{i}}(\mathbf{x}_A, t) + 2\omega_{\bar{i}}\rho\frac{3}{c^2}\mathbf{c}_{\bar{i}}\cdot\mathbf{u}_B \quad (6)$$

where $\bar{i}$ denotes the index for the opposite direction to $\mathbf{c}_i$ (i.e., $\mathbf{c}_{\bar{i}} = -\mathbf{c}_i$), and

$$g_{\bar{i}}(\mathbf{x}_A, t) = \omega_{\bar{i}}\rho(\mathbf{x}_A + \mathbf{c}_i\delta t)\Big(1 + \frac{3}{c^2}\mathbf{c}_{\bar{i}}\cdot\mathbf{u}_{bf} + \frac{9}{2c^4}(\mathbf{c}_{\bar{i}}\cdot\mathbf{u}_F)^2 - \frac{3}{2c^2}\mathbf{u}_F\cdot\mathbf{u}_F\Big) \quad (7)$$

is a fictitious equilibrium distribution function at the fluid node A. ω_i, $i = 0, 1, \ldots, Q-1$, are the weight factors of the LBM method. $\mathbf{u}_B = \mathbf{u}(\mathbf{x}_B, t)$ and $\mathbf{u}_F = \mathbf{u}(\mathbf{x}_F, t)$ are the boundary and fluid velocities respectively, with $\mathbf{x}_B$ the intersection point between the boundary and the link joining A with F. Different choices of $\mathbf{u}_{bf}$, a velocity between $\mathbf{u}_B$ and $\mathbf{u}_F$, give alternative values of the parameter χ, the weighting factor that controls the interpolation (or extrapolation). To improve numerical stability [22, 23] propose

$$\mathbf{u}_{bf} = \mathbf{u}_G = \mathbf{u}(\mathbf{x}_F + \mathbf{c}_i\delta t, t), \quad \chi = \frac{2\Delta - 1}{\tau - 2}, \quad \text{if } \Delta < \frac{1}{2},$$

and

$$\mathbf{u}_{bf} = \mathbf{u}_F + \frac{3}{2\Delta}(\mathbf{u}_B - \mathbf{u}_F), \quad \chi = \frac{2\Delta - 1}{\tau + \frac{1}{2}}, \quad \text{if } \Delta \geq \frac{1}{2},$$

where $0 \leq \Delta \leq 1$ is the fractional distance

$$\Delta = \frac{\|\mathbf{x}_F - \mathbf{x}_B\|}{\|\mathbf{x}_F - \mathbf{x}_A\|}. \quad (8)$$

When the body moves with respect to the lattice, there may be nodes in the body region at time t that become fluid nodes at time $t + \delta t$. It is then necessary to assign initial values to the variables at the new fluid nodes to evolve them. A practical way to do this is to evolve the nodes in the body region (solid nodes) so that they have values assigned when they become fluid nodes. There are more precise initializations for the variables at these nodes that change domain, like the one proposed in [10].

B. Forces evaluation in lattice Boltzmann method

It is of great interest to have a robust and accurate method to compute flow forces in fluid mechanics. Several algorithms have been proposed to carry out this in the context of LBM. Many of these procedures fall in one of the categories: stress integration (*SI*) or momentum exchange (*ME*). Stress integration is based on the classical hydrodynamic approach (see e.g., [2]). In the context of LBM, the computational performance of ME is higher than that of SI. In SI one needs to compute the stress tensor in all lattice nodes which are near neighbors of the body surface. One then needs to extrapolate the stress tensor to the surface, and finally obtain the total flow forces on the body as an integral over the whole body surface. In ME the procedure is simpler. The total force on the body is the sum of all contributions due to momentum change, in the directions pointing towards the body surface, over all boundary nodes. For a review of LBM applied flow force evaluation on suspended particles we refer to [1], section 6.

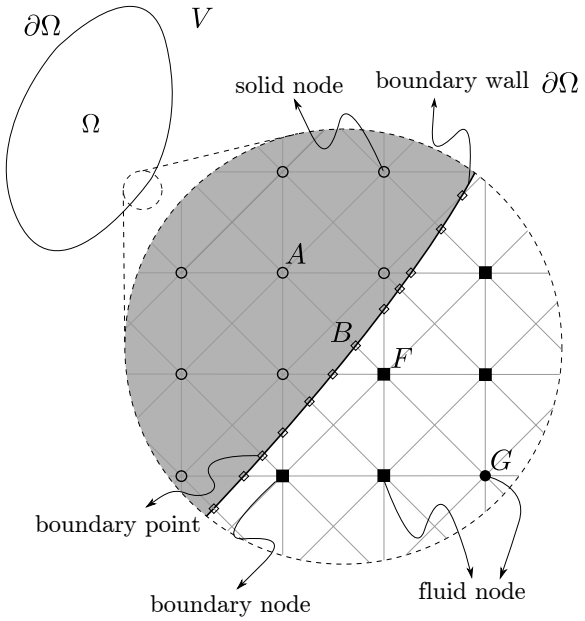

FIG. 1: Detail of boundary region, surrounding fluid and lattice.

In this section we write forces in general when we mean either force or torque. The idea of forces evaluation via momentum exchange in LBM was introduced by Ladd [5, 6] as a heuristic algorithm by thinking the flow as composed by "fluid particles" and using particle dynamics to describe their interaction with the boundaries. In this method, a particle suspension is defined as a shell where the same boundary condition procedure is applied for both interior and exterior fluid, using in all cases a midway bounce-back boundary condition. The forces evaluations are carried out considering the interior and exterior fluid.

Based in the works of Ladd, Aidun et. al. [7, 8] introduce some improvements to Ladd proposal, obtaining a robust method to analyze suspended solid particles with any solid-to-fluid density ratio. They also proposed a modified midway bounce-back as boundary condition,

and exclude the simulation of the interior fluid. The forces are evaluated considering the exterior fluid plus an impulsive contribution due to the nodes that are covered or uncovered when the body of interest move inside the fluid. In the case when the particles interact, as when they get close to contact, a particular model needs to be used as the one presented in [24].

Then, from the idea of momentum exchange, Mei et. al. [9] proposed a method to evaluate the fluid forces acting on a submerged body using a boundary condition method applied to arbitrary geometries. They exclude the simulation of the interior fluid as done in [8]. The direct application of this method to problems with moving bodies fails to obtain accurate forces evaluation as was shown in [4, 11]. Some proposals to improve the method presented in [9] for problems with moving bodies were made. Wen et. al. [11] presented one of this proposals. Their correction is based in the introduction of terms representing impulsive forces. Aidun et. al. [8] give an improved an accurate method in moving geometry problems.

The impulsive force terms introduced in [8] and [11], come from the nodes that are covered or uncovered when the body moves with respect to the lattice. This correction provoked some controversies, the main discussion being about some "noise" that appear in the evaluation of forces.

Based on the work of Mei et. al. [9], other approaches to evaluate forces in moving geometries, without the introduction of impulsive terms, were made. No rigorous proof was presented for these methods. Both [12] and [25] present a similar methods that are based in computing the momentum exchange in a reference frame comoving with the wall.

All the ME based methods cited here were specifically designed for LBM and have been implemented and tested in many fluid-mechanical problems. To the knowledge of the authors there is no formal derivation of them in the literature. The work of Caiazzo and Junk present an analysis of ME that uses an asymptotic expansion [26].

In this work we give a demonstration of ME, from a fluid mechanics perspective, in which some terms previously introduced as ad-hoc corrections appear naturally. In particular, we find that the corrections proposed in [11] and [8] are adequate when evaluating the force in a reference frame fixed to the lattice. In the spirit of our deduction of ME, we also deduce the alternative description presented in [12, 25], which is based on a reference frame comoving with the body.

III. MOMENTUM EXCHANGE METHOD

We want to simulate a fluid flow around a submerged body, within a region of space that we denote by V. We consider V to be a fixed region of space as seen on an inertial reference frame. We have covered V with a uniform constant lattice to solve the fluid motion by applying the lattice-Boltzmann method as described in section II.

The submerged body occupies a sub-region $\Omega(t) \subset V$ that we consider, along the whole simulation, strictly contained in V. As the time dependence indicates, $\Omega(t)$ doesn't need to be fixed. $\Omega(t)$ can move and could even change shape.

In this section we derive the force and torque that the flow applies on the body. The movement of the body is assumed to be prescribed along this derivation, i.e., Ω is a given function of t. During an actual computation the body movement is determined by integrating the equations of motion of the body simultaneously with the flow equations. The equations of motion of the body take into account the fluid force on the body, the bulk forces like weight, etc.

A. Reynolds transport theorem

For future reference we briefly remind here the Reynolds transport theorem. We consider first the case of a fluid system. Let $\Omega_S(t)$ denote a region that encloses a fluid system, that is a fixed material portion of the flow. In this case the velocity of the surface $\partial\Omega_S(t)$ at any point is precisely the fluid velocity at that point. Let $\boldsymbol{\eta}(\mathbf{x}, t)$ denote a (volume) density describing some property of the fluid (like mass density, momentum density, angular momentum density, etc.). The corresponding extensive property for the system is then

$$\mathbf{N}_S(t) = \int_{\Omega_S(t)} \boldsymbol{\eta}(\mathbf{x}, t)\, d\mathbf{x}.$$

The transport theorem states that

$$\frac{d\mathbf{N}_S}{dt} = \int_{\Omega_S(t)} \frac{\partial \boldsymbol{\eta}}{\partial t}\, d\mathbf{x} + \oint_{\partial\Omega_S(t)} \boldsymbol{\eta}\mathbf{u} \cdot \hat{n}\, dS. \qquad (9)$$

Here $\mathbf{u}$ denotes the fluid velocity, and $\hat{n}$ is the outward directed normal to the boundary $\partial\Omega_S$.

Now, let $\Omega_C(t)$ be a control volume (a region of fluid defined for convenience that does not necesarily move with the flow) with arbitrary movement, and let $\mathbf{v}(\mathbf{x}, t)$ denote the velocity of a point at the surface $\partial\Omega_C(t)$. In this case we have

$$\frac{d}{dt}\int_{\Omega_C(t)} \boldsymbol{\eta}\, d\mathbf{x} = \int_{\Omega_C(t)} \frac{\partial \boldsymbol{\eta}}{\partial t}\, d\mathbf{x} + \oint_{\partial\Omega_C(t)} \boldsymbol{\eta}\mathbf{v} \cdot \hat{n}\, dS. \quad (10)$$

Now, at a particular time of interest we choose a control volume $\Omega_C(t)$ which is coincident with a system volume $\Omega_S(t)$, but not in general at future times. That is $\Omega_C(t) = \Omega_S(t)$, but $\Omega_C(t') \neq \Omega_S(t')$, if $t' \neq t$. Then we can eliminate the first term on the right hand side in (9) by using (10) which gives,

$$\frac{d\mathbf{N}_S}{dt} = \frac{d}{dt}\int_{\Omega_C(t)} \boldsymbol{\eta}\, d\mathbf{x} + \oint_{\partial\Omega_C(t)} \boldsymbol{\eta}(\mathbf{u} - \mathbf{v}) \cdot \hat{n}\, dS. \quad (11)$$

Notice that $\mathbf{u} - \mathbf{v}$ measures the fluid velocity at a boundary point with respect to that boundary point.

We are interested in two particular cases. One of them is when $\mathbf{N} = \mathbf{P}$ is the total momentum contained in $\Omega_S(t)$, so that $\boldsymbol{\eta} = \rho(\mathbf{x}, t)\mathbf{u}(\mathbf{x}, t)$. The second case is when $\mathbf{N} = \mathbf{H}$ is the total angular momentum, with respect to a reference point $\mathbf{x}_0$, so that $\boldsymbol{\eta} = \mathbf{r}(\mathbf{x}) \times \rho(\mathbf{x}, t)\mathbf{u}(\mathbf{x}, t)$, with $\mathbf{r}(\mathbf{x}) = \mathbf{x} - \mathbf{x}_0$. The evaluation of equation (9) or (11) for the momentum and angular momentum cases give us the total force and torque applied over the fluid system contained in $\Omega_S(t) = \Omega_C(t)$.

The first term on the right hand side in (11) represents the total variation of $\boldsymbol{\eta}$ contained in the control volume $\Omega_C(t)$, while the second term in the right hand side is a surface integral that amounts the $\boldsymbol{\eta}$ flowing out of the volume $\Omega_C(t)$.

B. Derivation of momentum exchange

As explained in Section II A, the boundary conditions can be thought as an artificial flow inside Ω. This artificial flow is in turn decomposed into Q artificial flows, one for each fundamental velocity $\mathbf{c}_i$ in the method. To explain the effect of these flows we refer back to the figure 1. Consider the boundary node F and the direction $\mathbf{c}_i$ pointing from A to F. At every time step, the role of the boundary condition is to replace the value of $\hat{f}_i(\mathbf{x}_A, t)$ that would otherwise be provided by a collision step, by a new value. Altogether, these replacements carried out by the boundary condition are a way of introducing a certain amount of momentum in the i direction, at every time step. We derive ME by computing the amount of momentum that the boundary condition introduces per unit time. In this way we compute the force that each of these artificial flows apply to the external flow. The addition over all elementary directions i accounts for the total force the submerged body applies over the surrounding flow. By action-reaction principle, the force that the surrounding flow applies over the the submerged body is exactly the opposite.

We consider the system of particles associated to a lattice velocity $\mathbf{c}_i$ that at time t is exactly inside $\Omega(t)$. At $t + \delta t$ this system moved by an amount $\mathbf{c}_i \delta t$. We call $\mathcal{P}_{i,t}(t')$ the set of nodes associated to this system of particles at time t' and $\mathbf{P}_{i,t}(t')$ denotes its momentum at time t'. Finally we denote $\mathcal{A}_t$ the set of lattice nodes A inside $\Omega(t)$.

In the following subsections we derive the force and torque that the flow applies to the body through its surface. The cases of static and moving bodies are treated.

1. Force

The amount of momentum the boundary conditions add per unit time to the i-th system of particles is

$$\frac{d\mathbf{P}_{i,t}}{dt} = \frac{\mathbf{P}_{i,t}(t + \delta t) - \mathbf{P}_{i,t}(t)}{\delta t} + \mathcal{O}(\delta t) \qquad (12)$$

where

$$\mathbf{P}_{i,t}(t') = \delta x^D \sum_{A \in \mathcal{P}_{i,t}(t')} \mathbf{c}_i f_i(\mathbf{x}_A, t'). \qquad (13)$$

Neglecting $\mathcal{O}(\delta t)$ terms we have

$$\frac{d\mathbf{P}_{i,t}}{dt} \simeq \frac{\delta x^D}{\delta t}\Big(\sum_{A \in \mathcal{P}_{i,t}(t+\delta t)} \mathbf{c}_i f_i(\mathbf{x}_A, t + \delta t) - \sum_{A \in \mathcal{P}_{i,t}(t)} \mathbf{c}_i f_i(\mathbf{x}_A, t)\Big). \qquad (14)$$

2. Force on a static body

We assume first the case of a static body, so that Ω and the set $\mathcal{A}$ are constant in time. The first term in (14) can be rewritten in terms of the sets $\mathcal{G}_i$ of *gained* and $\mathcal{L}_i$ of *lost* nodes as a consequence of the displacement of the system of particles from t to $t + \delta t$. This displacement is exemplified in Figure 2 for the $D2Q9$ model and the directions $i = 1$ and $i = 5$.

To simplify notation we define $g_i = \mathbf{c}_i f_i(\mathbf{x}_A, t + \delta t)$. The first term in (14) becomes

$$\sum_{A \in \mathcal{P}_{i,t}(t+\delta t)} g_i = \sum_{A \in \mathcal{G}_i} g_i - \sum_{A \in \mathcal{L}_i} g_i + \sum_{A \in \mathcal{P}_{i,t}(t)} g_i \qquad (15)$$

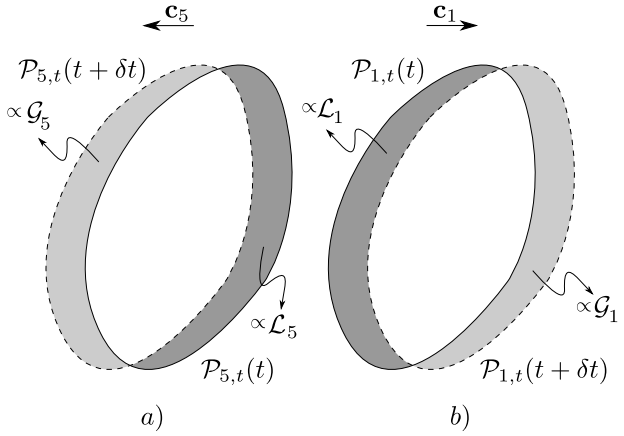

FIG. 2: Schematic diagram of the areas occupied by $\mathcal{P}_{i,t}(t)$ and $\mathcal{P}_{i,t}(t + \delta t)$ for $i = 1, 5$. The figure shows shaded areas proportional to the size of the sets $\mathcal{G}_i$ *gained* and $\mathcal{L}_i$ *lost* nodes when $\mathcal{P}_{i,t}(t)$ is displaced one lattice site in the $\mathbf{c}_5$ (scheme a) and $\mathbf{c}_1$ (scheme b) directions in the $D2Q9$ model.

Inserting this into (14) and adding over the Q systems we get the LBM approximation to the force introduced

by the boundary conditions.

$$\mathbf{F}_c(t) \simeq \delta x^D \sum_{i=0}^{Q-1} \sum_{A\in\mathcal{P}_{i,t}(t)} \mathbf{c}_i \frac{f_i(\mathbf{x}_A, t+\delta t) - f_i(\mathbf{x}_A, t)}{\delta t} + \frac{\delta x^D}{\delta t} \sum_{i=0}^{Q-1} \Big(\sum_{A\in\mathcal{G}_i} g_i - \sum_{A\in\mathcal{L}_i} g_i \Big) \quad (16)$$

We want to compare this expression with the Reynolds transport theorem (11) applied to the artificial flow inside $\Omega(t)$. The force introduced by the boundary conditions is the constraint force acting on the body to keep it at a fixed position. The first term in the right hand side of (16) is an LBM approximation of the volume term in (11). The second term in (16) is composed of sums on sets of nodes which are near neighbors of the boundary $\partial\Omega$. This second term is precisely the LBM approximation to the surface integral term in (11). As the interaction between the body and the surrounding fluid occurs only through the body's surface, this second term in (16) is the term we are interested in. By action-reaction principle the flow force on the body is,

$$\mathbf{F}_f(t) \simeq \frac{\delta x^D}{\delta t} \sum_{i=0}^{Q-1} \Big(- \sum_{A\in\mathcal{G}_i} g_i + \sum_{A\in\mathcal{L}_i} g_i \Big) \quad (17)$$

Notice that $A \in \mathcal{L}_i$ if and only if there is a node $B \in \mathcal{G}_{\bar{i}}$ such that $\mathbf{x}_A = \mathbf{x}_B + \mathbf{c}_i\delta t$. Therefore

$$\mathbf{F}_f(t) \simeq \frac{\delta x^D}{\delta t} \sum_{i=0}^{Q-1} \Big(- \sum_{A\in\mathcal{G}_i} \mathbf{c}_i f_i(\mathbf{x}_A, t+\delta t) + \sum_{A\in\mathcal{G}_{\bar{i}}} \mathbf{c}_i f_i(\mathbf{x}_A + \mathbf{c}_i\delta t, t+\delta t) \Big)$$

Now, a sum over all sets $\mathcal{G}_{\bar{i}}$ can be written as a sum over all sets $\mathcal{G}_i$, we obtain

$$\mathbf{F}_f(t) \simeq -\frac{\delta x^D}{\delta t} \sum_{i=0}^{Q-1} \sum_{A\in\mathcal{G}_i} \mathbf{c}_i \Big(f_i(\mathbf{x}_A, t+\delta t) + f_{\bar{i}}(\mathbf{x}_A + \mathbf{c}_{\bar{i}}\delta t, t+\delta t) \Big). \quad (18)$$

We notice that

$$f_{\bar{i}}(\mathbf{x}_A + \mathbf{c}_{\bar{i}}\delta t, t+\delta t) = \hat{f}_{\bar{i}}(\mathbf{x}_A, t), \qquad f_i(\mathbf{x}_A, t+\delta t) = \hat{f}_i(\mathbf{x}_A - \mathbf{c}_i\delta t, t). \quad (19)$$

The first identity is the streaming step from the outer nodes in a direction that points into Ω (across the boundary). This values of $\hat{f}_i$ are provided by the collision step. The second identity is a streaming step from inner nodes in a direction pointing outwards (across the boundary); these value of $\hat{f}_i$ are provided by the boundary condition. The flow force on the submerged body can then be written as

$$\mathbf{F}_f(t) \simeq -\frac{\delta x^D}{\delta t} \sum_{i=0}^{Q-1} \sum_{A\in\mathcal{G}_i} \mathbf{c}_i \big(\hat{f}_i(\mathbf{x}_A - \mathbf{c}_i\delta t, t) + \hat{f}_{\bar{i}}(\mathbf{x}_A, t) \big). \quad (20)$$

To compare the equation (20) with the equivalent ones in the literature, care has to be taken as regards different definitions of the sets $\mathcal{G}_i$. Equation (20) is precisely the expression that appears extensively in the literature [4, 8, 9, 11] as the momentum exchange method to evaluate forces in static bodies.

3. Force on a moving body

For the case of a moving body we derive two alternative methods for evaluating the flow force. In this way we recover the two main proposals that appear in the literature.

The first derivation shows that the proposals presented in [8, 11] are adequate formulations to get flow force on moving bodies. To the knowledge of the authors, the correctness and accuracy of these proposals were studied before only via benchmark numerical tests. The second derivation shows that the method presented in [12, 25] is also adequate to evaluate forces in moving submerged bodies.

When the submerged body is moving, the region $\Omega(t)$ and the set of lattice nodes $\mathcal{A}_t$ are no longer constant. For some time steps, one can even expect the set of nodes $\mathcal{A}_{t+\delta t}$ to be the same as the set of nodes $\mathcal{A}_t$. In any case it is useful define the sets of nodes $\mathcal{A}_t^+$ and $\mathcal{A}_t^-$ as

$$A \in \mathcal{A}_t^+, \quad \text{if} \quad A \in \mathcal{A}_{t+\delta t} \quad \text{and} \quad A \notin \mathcal{A}_t,$$
$$A \in \mathcal{A}_t^-, \quad \text{if} \quad A \in \mathcal{A}_t \quad \text{and} \quad A \notin \mathcal{A}_{t+\delta t}.$$

Figure 3 shows a scheme of a typical situation when the body moves.

The expression (15) is still valid in this case. However, at time $t+\delta t$ we want to make reference to the body's new position, so we rewrite the term that sums over $\mathcal{P}_{i,t}(t)$ as

$$\sum_{A\in\mathcal{P}_{i,t}(t)} g_i = \sum_{A\in\mathcal{A}_{t+\delta t}} g_i + \sum_{A\in\mathcal{A}_t^-} g_i - \sum_{A\in\mathcal{A}_t^+} g_i \quad (21)$$

a. Force on a moving body: method 1. We insert (21) into (15) and use the result into (14). Then we add over i to get an approximation of the flow force acting on the body Ω

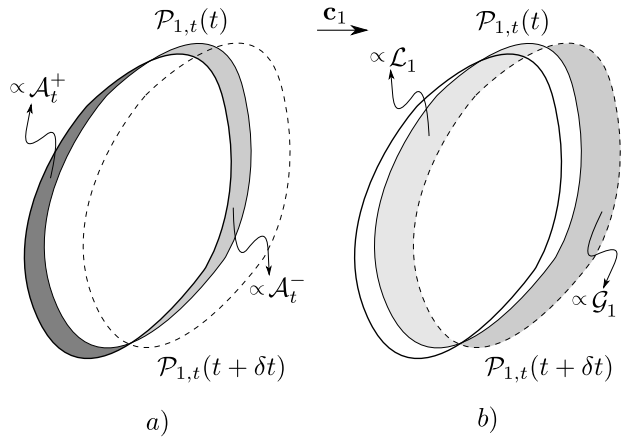

FIG. 3: Schematic diagram of the area occupied by the nodes $\mathcal{P}_{1,t}(t)$ and $\mathcal{P}_{1,t}(t+\delta t)$. The figure shows shaded areas proportional to the size of the lattice nodes $\mathcal{A}_t^+$ and $\mathcal{A}_t^-$ (scheme a), and $\mathcal{G}_1$ and $\mathcal{L}_1$ (scheme b) as defined in the text.

$$\mathbf{F}_f(t) \simeq \frac{\delta x^D}{\delta t}\sum_{i=0}^{Q-1}\Big(-\sum_{A\in\mathcal{G}_i}\mathbf{c}_i\big(\hat{f}_i(\mathbf{x}_A-\mathbf{c}_i\delta t,t)+\hat{f}_{\bar{i}}(\mathbf{x}_A,t)\big) - \sum_{A\in\mathcal{A}_t^-}\mathbf{c}_i f_i(\mathbf{x}_A,t+\delta t)+\sum_{A\in\mathcal{A}_t^+}\mathbf{c}_i f_i(\mathbf{x}_A,t+\delta t)\Big). \quad (22)$$

Where again, as we are looking for the surface contributions to the force, we dropped the volume contribution. Equation (22) shows a main term, which is the same as in the case of a static body, representing the particle's exchange of momentum across the boundary, but now this term is corrected by the last two terms which accounts for the momentum associated to the nodes that enter or leave $\Omega(t)$ as a consequence of the body movement. In this way we obtain terms similar to that proposed by Aidun et. al. [8] to evaluate the force on a moving body. We show that these terms are correct and necessary to obtain the complete superficial contribution to the force when the body moves. Equation (22) is then similar to that introduced in [8] and by Wen et. al. [11], extensively used in the literature to evaluate the fluid force on moving bodies.

There is a minor difference between the expression (22) and those introduced in [8] and [11]. In their cases, the force at time t considers the lattice nodes that enter and leave $\Omega(t)$ between $t-\delta t$ and t (i.e., backward in time). In our case, (22) requires to know the sets $\mathcal{A}^+$ and $\mathcal{A}^-$, that is the sets of nodes that enter and leave Ω between t and $t+\delta t$ (i.e., forward in time). The determination of the sets $\mathcal{A}^+$ and $\mathcal{A}^-$ is direct if the movement of the body is given (predetermined) at all times, in this case (22) is an explicit expression. If, however, the motion of the body is to be computed simultaneously with the flow, the equation (22) becomes implicit. In this last case it is convenient to use an approximation to determine $\mathcal{A}^+$ and $\mathcal{A}^-$ so that the equation becomes explicit.

In the numerical tests in section IV, we implement two different approximations to find the sets $\mathcal{A}^+$ and $\mathcal{A}^-$. Both approximations work well, giving no appreciable difference in the outcomes of the benchmark tests. The first approximation is the procedure proposed in [8]. The second approximation is more complicated. It computes the sets $\mathcal{A}^+$ and $\mathcal{A}^-$ by approximating the region $\Omega(t+\delta t)$ as if it was moving with the speed computed at the previous time step. With this information the flow force can be computed at time t and then the correct displacement of Ω from t to $t+\delta t$ recomputed. Though computationally more expensive, as two displacements of Ω are computed at each time step, this second approximation is more precise than the first one and may be worth using it in some situations.

Notice that the variables associated to the lattice nodes belonging to $\mathcal{A}^-$ do not have values assigned at time t since these nodes enter the fluid region between t and $t+\delta t$. These values are needed in order to compute the time step from t to $t+\delta t$. As mentioned previously, various rules to "initialize" these variables are proposed in the literature. In our simulations we implement the proposals given in [10] and [8]. Also we implement a method that sets the mentioned variables by using the equilibrium distribution function, where the macroscopic variables are set as an average of the values at the nearest neighbor fluid nodes. The evaluation of the force by (22) we present in Section IV show a short time scale noise. The use of the first two methods mentioned before to initialize the nodes that enter the fluid region present lower noise level.

The main sources of "noise" in the force evaluation using (22) are the impulsive nature of the additional terms related to $\mathcal{A}^+$ and $\mathcal{A}^-$. This noise has been observed before.

A last observation is that (22) is not Galilean invariant. In [27] the authors present a correction to obtain Galilean invariance of the force evaluation method proposed in [8] which, as mentioned before, is similar to (22).

b. Force on a moving body: method 2. In [12, 25] the authors show an alternative method to avoid the undesirable noise effect in the force evaluation. The derivation of this method is based on the fact that the time derivative of a particle's momentum is independent of the inertial frame used to compute it.

The momentum of a fluid element around $\mathbf{x}$, when seen on an inertial reference frame that moves with velocity $\mathbf{v}$ with respect to the lattice is written in LBM as the superposition of Q contributions of the form $(\mathbf{c}_i-\mathbf{v})f_i(\mathbf{x},t)$. To evaluate (12) we choose for each node $A\in\mathcal{P}_{i,t}(t)$, a convenient inertial reference frame whose velocity with respect to the lattice is denoted by $\mathbf{v}(\mathbf{x}_A,t)$. For each particle we need, of course, to keep the same reference frame along the time lapse of the approximation $(t,t+\delta t)$. Therefore, the amount of momentum per unit time the boundary conditions add to the i-th system of particles

between t and $t+\delta t$, can be written as

$$\frac{d\hat{\mathbf{P}}_{i,t}}{dt} \simeq \frac{\delta x^D}{\delta t}\Big(\sum_{A\in\mathcal{P}_{i,t}(t+\delta t)} \big(\mathbf{c}_i - \mathbf{v}(\mathbf{x}_A - \mathbf{c}_i\delta t, t)\big) f_i(\mathbf{x}_A, t+\delta t) - \sum_{A\in\mathcal{P}_{i,t}(t)} \big(\mathbf{c}_i - \mathbf{v}(\mathbf{x}_A, t)\big) f_i(\mathbf{x}_A, t)\Big). \quad (23)$$

It is convenient to emphasize here that the fluid flow (i.e., the f_i's) is always computed in the inertial reference frame in which the lattice is fixed.

Now, in analogy with (15), we can decompose the first sum in (23) as

$$\sum_{A\in\mathcal{P}_{i,t}(t+\delta t)} \hat{g}_i = \sum_{A\in\mathcal{P}_{i,t}(t)} \hat{g}_i + \sum_{A\in\mathcal{G}_i} \hat{g}_i - \sum_{A\in\mathcal{L}_i} \hat{g}_i \quad (24)$$

where $\hat{g}_i = \big(\mathbf{c}_i - \mathbf{v}(\mathbf{x}_A - \mathbf{c}_i\delta t, t)\big) f_i(\mathbf{x}_A, t+\delta t)$. The last sum over $\mathcal{L}_i$ can be expressed as sum over $\mathcal{G}_{\bar{i}}$, and the first sum in (24) can be split as in (21). The velocities of the reference frames for nodes in $\mathcal{L}_i$ come from nodes outside $\mathcal{P}_{i,t}(t)$. We chose $\mathbf{v}(\mathbf{x}_A - \mathbf{c}_i\delta t, t) = \mathbf{v}(\mathbf{x}_A, t)$ for $A \in \mathcal{L}_i$. Using all this in (23), summing over i and keeping only the surface terms gives minus the flow force

$$\mathbf{F}_f \simeq \frac{\delta x^D}{\delta t} \sum_{i=0}^{Q-1} \Big[\sum_{A\in\mathcal{A}_t^+} \hat{g}_i - \sum_{A\in\mathcal{A}_t^-} \hat{g}_i - \sum_{A\in\mathcal{G}_i} \Big(\big(\mathbf{c}_i - \mathbf{v}(\mathbf{x}_A - \mathbf{c}_i\delta t, t)\big) f_i(\mathbf{x}_A, t+\delta t) - \big(\mathbf{c}_{\bar{i}} - \mathbf{v}(\mathbf{x}_A - \mathbf{c}_i\delta t, t)\big) f_{\bar{i}}(\mathbf{x}_A - \mathbf{c}_{\bar{i}}\delta t, t+\delta t)\Big)\Big]. \quad (25)$$

Now we make an specific choice for the frames used at the nodes in $\mathcal{P}_{i,t}(t)$ close to the boundary. We set $\mathbf{v}(\mathbf{x}_A, t)$ as the average velocity of the boundary points (see Figure 1) corresponding to $\mathbf{x}_A$. With this choice, the first two terms in the right hand side of (25) are negligible since both $\sum_{i=0}^{Q-1} \mathbf{c}_i f_i$ and $\sum_{i=0}^{Q-1} \mathbf{v}(\mathbf{x}_A - \mathbf{c}_i\delta t, t) f_i(\mathbf{x}_A, t+\delta t)$ represent close approximations to $\rho\mathbf{u}$ at the boundary. Other nodes not close to the boundary contribute only to the volume term which is dropped, and therefore the choice of the reference frames is unimportant. The result obtained in this way is an LBM discretization of the surface term in the right hand side of (11).

$$\mathbf{F}_f = -\frac{\delta x^D}{\delta t} \sum_{i=0}^{Q-1} \sum_{A\in\mathcal{G}_i} \Big(\big(\mathbf{c}_i - \mathbf{v}(\mathbf{x}_A - \mathbf{c}_i\delta t, t)\big) \hat{f}_i(\mathbf{x}_A - \mathbf{c}_i\delta t, t) - \big(\mathbf{c}_{\bar{i}} - \mathbf{v}(\mathbf{x}_A - \mathbf{c}_i\delta t, t)\big) \hat{f}_{\bar{i}}(\mathbf{x}_A, t)\Big) \quad (26)$$

The method used in [12, 25], instead of choosing a unique frame for each node $\mathbf{x}_A \in \mathcal{P}_{i,t}(t)$ close to the boundary, choose a different frame for each direction i pointing to the boundary. This constitutes an approximation to (26) given by

$$\mathbf{F}_f = -\frac{\delta x^D}{\delta t} \sum_{i=0}^{Q-1} \sum_{A\in\mathcal{G}_i} \Big(\big(\mathbf{c}_i - \mathbf{v}_{A,i}(t)\big) \hat{f}_i(\mathbf{x}_A - \mathbf{c}_i\delta t, t) - \big(\mathbf{c}_{\bar{i}} - \mathbf{v}_{A,i}(t)\big) \hat{f}_{\bar{i}}(\mathbf{x}_A, t)\Big) \quad (27)$$

where $\mathbf{v}_{A,i}(t)$ is the velocity of the boundary point of $\mathbf{x}_A$ in the direction i. In [12] the authors numerically test this approximation and show that equation (27) is Galilean invariant.

Either expressions (22) and (26) are correct expressions, they constitute different approximations of the flow force. The later has some advantages though. First, it is computationally more efficient, since it is not necessary to determine the sets $\mathcal{A}_t^+$ and $\mathcal{A}_t^-$. As a result the method is always explicit and it presents a notorious noise decrease in force evaluation as shown in [12] for the approximation (27).

4. *Torque*

The derivation of the torque acting on the submerged body is analogous to that of the force. The angular momentum per unit time introduced by the i-th artificial flow is

$$\frac{d\mathbf{H}_{i,t}}{dt} = \frac{\mathbf{H}_{i,t}(t+\delta t) - \mathbf{H}_{i,t}(t)}{\delta t} + \mathcal{O}(\delta t) \quad (28)$$

where

$$\mathbf{H}_{i,t}(t') = \delta x^D \sum_{A\in\mathcal{P}_{i,t}(t')} \mathbf{r}(\mathbf{x}_A) \times \mathbf{c}_i f_i(\mathbf{x}_A, t'), \quad (29)$$

with $\mathbf{r}(\mathbf{x}_A) = \mathbf{x}_A - \mathbf{x}_0$, $\mathbf{H}_{i,t}(t')$ is the angular momentum of the particle system at time t' with respect to a fixed point $\mathbf{x}_0$. Neglecting $\mathcal{O}(\delta t)$ terms in equation (28) we have

$$\frac{d\mathbf{H}_{i,t}}{dt} \simeq \frac{\delta x^D}{\delta t}\Big(\sum_{A\in\mathcal{P}_{i,t}(t+\delta t)} \mathbf{r}(\mathbf{x}_A)\times\mathbf{c}_i f_i(\mathbf{x}_A, t+\delta t) - \sum_{A\in\mathcal{P}_{i,t}(t)} \mathbf{r}(\mathbf{x}_A)\times\mathbf{c}_i f_i(\mathbf{x}_A, t)\Big). \quad (30)$$

As we have done in section III B 1, we treat the case of a static body first and then extend the proposal to the case of a moving body.

5. Torque on static body

Using the lattice node sets $\mathcal{G}_i$ and $\mathcal{L}_i$ (shown in Figure 2) to rewrite the first term in (30), and denoting $h_i = \mathbf{r}(\mathbf{x}_A)\times\mathbf{c}_i f_i(\mathbf{x}_A, t+\delta t)$ for simplicity, we have

$$\sum_{A\in\mathcal{P}_{i,t}(t+\delta t)} h_i = \sum_{A\in\mathcal{P}_{i,t}(t)} h_i + \sum_{A\in\mathcal{G}_i} h_i - \sum_{A\in\mathcal{L}_i} h_i \quad (31)$$

Inserting this into (30) and adding over the Q systems we get an approximation to the constraint torque acting on Ω,

$$\mathbf{T}_c(t) \simeq \delta x^D \sum_{i=0}^{Q-1} \sum_{A\in\mathcal{P}_{i,t}(t)} \mathbf{r}(\mathbf{x}_A)\times\mathbf{c}_i \frac{f_i(\mathbf{x}_A, t+\delta t) - f_i(\mathbf{x}_A, t)}{\delta t} + \frac{\delta x^D}{\delta t}\sum_{i=0}^{Q-1}\Big(\sum_{A\in\mathcal{G}_i} h_i - \sum_{A\in\mathcal{L}_i} h_i\Big) \quad (32)$$

As in the force case, we can compare this expression with the Reynolds Transport theorem, then keeping just the approximation of the surface term in (11), we get an expression for the torque that the flow applies on the body,

$$\mathbf{T}_f(t) \simeq \frac{\delta x^D}{\delta t}\sum_{i=0}^{Q-1}\Big(-\sum_{A\in\mathcal{G}_i} h_i + \sum_{A\in\mathcal{L}_i} h_i\Big) \quad (33)$$

Recalling the relation between $\mathbf{x}_A \in \mathcal{L}_i$ and $\mathbf{x}_B \in \mathcal{G}^{\bar{i}}$ ($\mathbf{x}_A = \mathbf{x}_B + \mathbf{c}_i\delta t$), and using (19)

$$\mathbf{T}_f \simeq -\frac{\delta x^D}{\delta t}\sum_{i=0}^{Q-1}\sum_{A\in\mathcal{G}_i}\Big(\mathbf{r}(\mathbf{x}_A)\times\mathbf{c}_i\big(\hat{f}_i(\mathbf{x}_A - \mathbf{c}_i\delta t, t) + \hat{f}_{\bar{i}}(\mathbf{x}_A, t)\big)\Big) \quad (34)$$

This equation is the expression that appears in the literature [4, 8, 9, 11] extensively as the momentum exchange method to evaluate torque on static bodies.

6. Torque on a moving body

In this section we follow a procedure and reasoning analogous to that of section III B 3. As with the force on a moving body we present two derivations that provide alternative methods to compute the torque.

We rewrite the first term on the right hand side of (31) to get the correct surface contribution when the surface moves,

$$\sum_{A\in\mathcal{P}_{i,t}(t)} h_i = \sum_{A\in\mathcal{A}_{t+\delta t}} h_i + \sum_{A\in\mathcal{A}_t^-} h_i - \sum_{A\in\mathcal{A}_t^+} h_i \quad (35)$$

a. Torque on a moving body: method 1. We replace (35) in (31), then from equation (30) and adding over the Q systems we obtain an approximation of the constraint torque acting on the body at time t. Thus the flow torque on a moving body turns out to be

$$\mathbf{T}_f(t) \simeq -\frac{\delta x^D}{\delta t}\sum_{i=0}^{Q-1}\Big(\sum_{A\in\mathcal{A}_t^-} h_i - \sum_{A\in\mathcal{A}_t^+} h_i + \sum_{A\in\mathcal{G}_i} \mathbf{r}(\mathbf{x}_A)\times\mathbf{c}_i\big(\hat{f}_i(\mathbf{x}_A - \mathbf{c}_i\delta t, t) + \hat{f}_{\bar{i}}(\mathbf{x}_A, t)\big)\Big). \quad (36)$$

Where we have used the relation of sets $\mathcal{G}_i$ and $\mathcal{L}_i$, and the equalities (19).

The equation (36) has two distinct contribution to the flow torque on $\Omega(t)$. The first one, is the contribution to the torque by the lattice nodes that enter and leave $\Omega(t)$ as a consequence of its displacement to $\Omega(t+\delta t)$. This contribution is composed by impulsive terms as we have noted in section III B 3. The second is the contribution due to the exchange of momentum across the boundary as a consequence of the displacement of the particle system from t to $t+\delta t$.

Expression (36) is similar to the one presented in the literature to evaluate the flow torque on moving bodies. This expression naturally introduces the ad-hoc correction terms first presented in [8] and used in [11].

As with the force, a difference between our proposal and those in the literature is the time at which the sets of lattice nodes $\mathcal{A}_t^+$ and $\mathcal{A}_t^-$ are evaluated. To avoid implicit expressions when the body movement is not predefined, we use some approximation methods, presented in section III B 3, to approach $\mathcal{A}_t^+$ and $\mathcal{A}_t^-$.

As one could expect, some short time scale noise in the torque computation appears as a consequence of the lattice nodes that enter and leave the fluid domain as the body moves.

b. Torque on a moving body: method 2. As with the force derivation, we also obtain an alternative derivation for the torque by considering the time derivatives of the angular momentum in different reference frames for each particle. The reference frames to compute the torque on the boundary nodes are chosen with a common origin $\mathbf{x}_0(t)$ and different velocities chosen as in the derivation of (26). We now define $\mathbf{r}(\mathbf{x}_A, t) = \mathbf{x}_A - \mathbf{x}_0(t)$, where $\mathbf{x}_0(t)$ is the origin of the moving inertial reference frames at time t. The amount of angular momentum the boundary conditions add per unit time to the i-th particle system is

$$\frac{d\hat{\mathbf{H}}_{i,t}}{dt} \simeq \frac{\delta x^D}{\delta t}\Big(\sum_{A\in\mathcal{P}_{i,t}(t+\delta t)} (\mathbf{r}(\mathbf{x}_A, t+\delta t) \times \big(\mathbf{c}_i - \mathbf{v}(\mathbf{x}_A - \mathbf{c}_i\delta t, t)\big) f_i(\mathbf{x}_A, t+\delta t) - \sum_{A\in\mathcal{P}_{i,t}(t)} \mathbf{r}(\mathbf{x}_A, t) \times \big(\mathbf{c}_i - \mathbf{v}(\mathbf{x}_A, t)\big) f_i(\mathbf{x}_A, t)\Big). \quad (37)$$

With

$$\begin{aligned}\mathbf{r}(\mathbf{x}_A, t+\delta t) =& \mathbf{x}_A - \mathbf{x}_0(t) - \mathbf{v}(\mathbf{x}_A - \mathbf{c}_i\delta t, t)\delta t \\ =& \mathbf{r}(\mathbf{x}_A, t) - \mathbf{c}_i\delta t + \big(\mathbf{c}_i - \mathbf{v}(\mathbf{x}_A - \mathbf{c}_i\delta t, t)\big)\delta t,\end{aligned}$$

where the last term does not contribute to (37) because of the vector product.

From equation (37), using (31) and (35), with h_i replaced by $\hat{h}_i = \big(\mathbf{r}(\mathbf{x}_A, t) - \mathbf{c}_i\delta t\big) \times \big(\mathbf{c}_i - \mathbf{v}(\mathbf{x}_A - \mathbf{c}_i\delta t, t)\big) f_i(\mathbf{x}_A, t+\delta t)$ give, adding over the Q systems and considering only the surface terms, an approximation of the flow torque acting on the body at time t.

$$\begin{aligned}\mathbf{T}_f(t) \simeq -\frac{\delta x^D}{\delta t}\sum_{i=0}^{Q-1}\Big(\sum_{A\in\mathcal{A}_t^-} \hat{h}_i - \sum_{A\in\mathcal{A}_t^+} \hat{h}_i + \\ \sum_{A\in\mathcal{G}_i} \big[\big(\mathbf{r}(\mathbf{x}_A, t) - \mathbf{c}_i\delta t\big) \times \big(\mathbf{c}_i - \mathbf{v}(\mathbf{x}_A - \mathbf{c}_i\delta t, t)\big) \hat{f}_i(\mathbf{x}_A - \mathbf{c}_i\delta t, t) \\ - \mathbf{r}(\mathbf{x}_A, t) \times \big(\mathbf{c}_{\bar{i}} - \mathbf{v}(\mathbf{x}_A - \mathbf{c}_i\delta t, t)\big) \hat{f}_{\bar{i}}(\mathbf{x}_A, t)\big]\Big). \quad (38)\end{aligned}$$

As with the force, the first two terms are negligible. Dropping these terms, the expression becomes explicit. As in the method 2 of force evaluation, instead of taking a unique frame for each node $\mathbf{x}_A \in \mathcal{P}_{i,t}(t)$ close to the boundary one can take different frames for each direction i pointing to the boundary. The resulting approximation is

$$\mathbf{T}_f(t) \simeq -\frac{\delta x^D}{\delta t}\sum_{i=0}^{Q-1}\Big(\sum_{A\in\mathcal{G}_i} \big[\big(\mathbf{r}(\mathbf{x}_A, t) - \mathbf{c}_i\delta t\big) \times \big(\mathbf{c}_i - \mathbf{v}_{A,i}(t)\big) \hat{f}_i(\mathbf{x}_A - \mathbf{c}_i\delta t, t) - \mathbf{r}(\mathbf{x}_A, t) \times \big(\mathbf{c}_{\bar{i}} - \mathbf{v}_{A,i}(t)\big) \hat{f}_{\bar{i}}(\mathbf{x}_A, t)\big]\Big). \quad (39)$$

where $\mathbf{v}_{A,i}(t)$ is the velocity of the boundary point of $\mathbf{x}_A$ in the direction i. Notice that the expression presented in [12, 25] can be obtained from (39) if the factor $\big(\mathbf{r}(\mathbf{x}_A, t) - \mathbf{c}_i\delta t\big)$ in the first cross product is approximated by $\mathbf{r}(\mathbf{x}_A, t)$.

IV. NUMERICAL TESTS

In this section we compare the results obtained with the expressions derived in section III to compute the force and torque acting on a submerged body. To this end we perform two benchmark tests on well known problems

that have been tested and benchmarked widely with others computational fluid dynamics methods, such as finite element method and finite difference methods.

We are interested in analyzing the dynamics of single bodies sedimenting along a vertical channel filled with a Newtonian fluid. The bodies are either circular or elliptic discs. The accuracy in the determination of the force and torque acting on the falling body directly affects the body's movement. If the force and torque are computed correctly, the displacement and rotation of the bodies along the domain should be in agreement with data presented in the literature [3, 4, 11, 28].

To solve the flow we use a *D2Q9* lattice scheme and SRT with $\tau = 0.6$. We use in our simulations the quasi-incompressible model. To check that the quasi incompressibility does not introduce artifacts in our simulation we repeated some of them with a compressible model and observed no discrepancies in the results. The fluid density and the kinematic viscosity are set to $\rho_f = 1000\,\mathrm{kg/m^3}$ and $\nu = 1 \times 10^{-6}\,\mathrm{m^2/s}$ respectively. The fluid is initially at rest and has zero velocity at the horizontal and vertical boundaries at all times. We implement these boundary conditions with the method presented in [29]. The acceleration of gravity acting on the body is $g = 9.81\,\mathrm{m/s^2}$ downwards.

The motion of each body is determined by integrating Newton's equation of motion, where the force is given by the fluid flow force, weight and buoyancy force and the torque is given by the flow torque. To integrate in time we use Euler Forward numerical scheme, which is first order accurate as the LBM method itself. We have also implemented two step (Adams-Bashforth) integration in time and noticed no appreciable difference in the results.

A. Sedimentation of a circular disc

In this benchmark test we analyze the dynamics of a single two-dimensional disc sedimenting along a vertical channel, shown schematically in Figure 4. We test the dynamics of the disc for two density relations $r_\rho = \rho_b/\rho_f$, with ρ_b and ρ_f the densities of the body (disc) and the fluid respectively.

The dimensions of the vertical channel are $W = 4d$ and $H = 8W$; the disc diameter is $d = 1 \times 10^{-3}\,\mathrm{m}$. The disc center is initially placed at $(x, y) = (7.6 \times 10^{-4}, 0)\,\mathrm{m}$ with the coordinate origin at $2.5 \times 10^{-2}\,\mathrm{m}$ from the bottom of the channel and placed as shown in Figure 4. We discretized the computational domain with $n_x \times n_y = 135 \times 1073$ lattice points.

We test the performance of the method for two density ratios $r_\rho = 1.01$, and 1.03. In Figures 6 and 7 we show the horizontal and vertical velocities and the trajectory of the center of the disc and the rotation angle of the disc as functions of time, for $r_\rho = 1.01$ and $r_\rho = 1.03$.

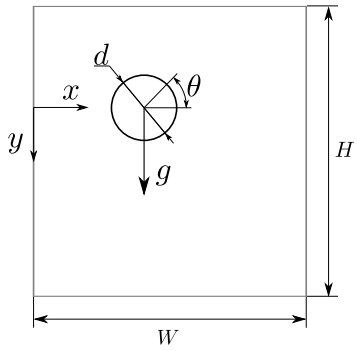

FIG. 4: An schematic diagram of the sedimentation disc problem.

When the disc is released from the initial position at $t = 0$, it starts moving and rotating along the channel. As one can see in the figures 6 and 7, the movement of the disc can be divided into two regimes: A transient and a stationary regime.

We compare results we obtained using a classical ME (20),(34) and the corrected methods given by (22), (36) and (27), (39). These results, particularly those obtained with the corrected methods are in good agreement with tests presented in [4] (obtained using LBM with SI), [11] (obtained using LBM with an expression similar to (22), (36)) and [28] (obtained using FEM). We observe visible discrepancies between the classical and the corrected methods for the horizontal velocity and position. The major discrepancy shows in the transient regime; no significant discrepancies can be seen in the stationary regime. Similar observations have been made by Wen et. al. [11] and Li et. al [4].

B. Sedimentation of an elliptic disc

In this section we present a benchmark test, similar to the previous one, where the circular disc is replaced with an elliptical disc, also sedimenting in a vertical channel filled with Newtonian fluid. This test is also widely analyzed in the literature. We study a problem as the one presented by Xia et. al. [3], where the authors use LBM and SI to obtain the forces on the body.

We show in Figure 5 a schematic diagram of the problem. We define three dimensionless parameters that characterize the problem. These parameters are the aspect ratio $\alpha = a/b$, with a and b the major and minor axes of the ellipse respectively, the blockage ratio $\beta = W/a$, with W the width of the vertical channel, and the density ratio r_ρ as defined in Section IV A.

An exhaustive analysis of this sedimentation problem was carried out by Xia et. al. [3]. They studied the influence on the dynamics of the density ratio, the aspect ratio, and the channel blockage ratio. For simplicity we analyze this problem with a fix blockage ratio, chosen so that we don't need to consider the wall-particle interac-

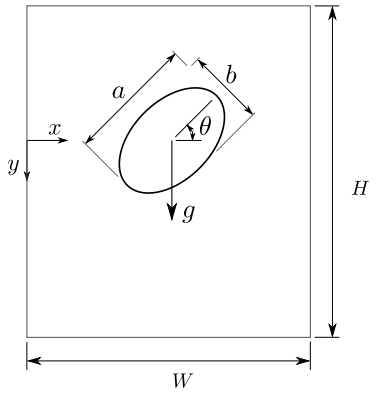

FIG. 5: An schematic diagram of the two-dimensional elliptical particle sedimenting in a vertical channel.

tion. Our interest is to test the method proposed in the present work, not to give a complete description of the sedimentation problem. We carry out simulations with a fixed geometrical configuration.

In our tests we use major axis $a = 10^{-3}$m, aspect ratio $\alpha = 2$ and blockage ratio $\beta = 4.0$. The properties of the fluid are the same used in Section IV A. Initially, the fluid is at rest, the center of the ellipse is placed at $(x, y) = (0.5W, 0)$m. The coordinate origin at 4.8×10^{-2}m from the bottom of the vertical channel. To break the symmetry of the problem, we choose an initial angular position $\theta_0 = \frac{\pi}{4}$. We set, following [3], a height $H = 50a$ and a width $W = 4a$. The domain is discretized in a lattice with $n_x \times n_y = 135 \times 1676$ points and density ratio is $r_\rho = 1.10$.

In the Figure 8 we show the dynamical variables given as a function of time and the complete trajectory of the ellipse computed using a classical ME (20),(34) and the corrected methods given by (22), (36) and (27), (39). Our results using the corrected methods are in good agreement with the results of Xia et. al. [3]. It is clear from Figure 8, that there exists an important difference, in the transient regime, and a minor difference in the final horizontal position between the corrected and uncorrected methods.

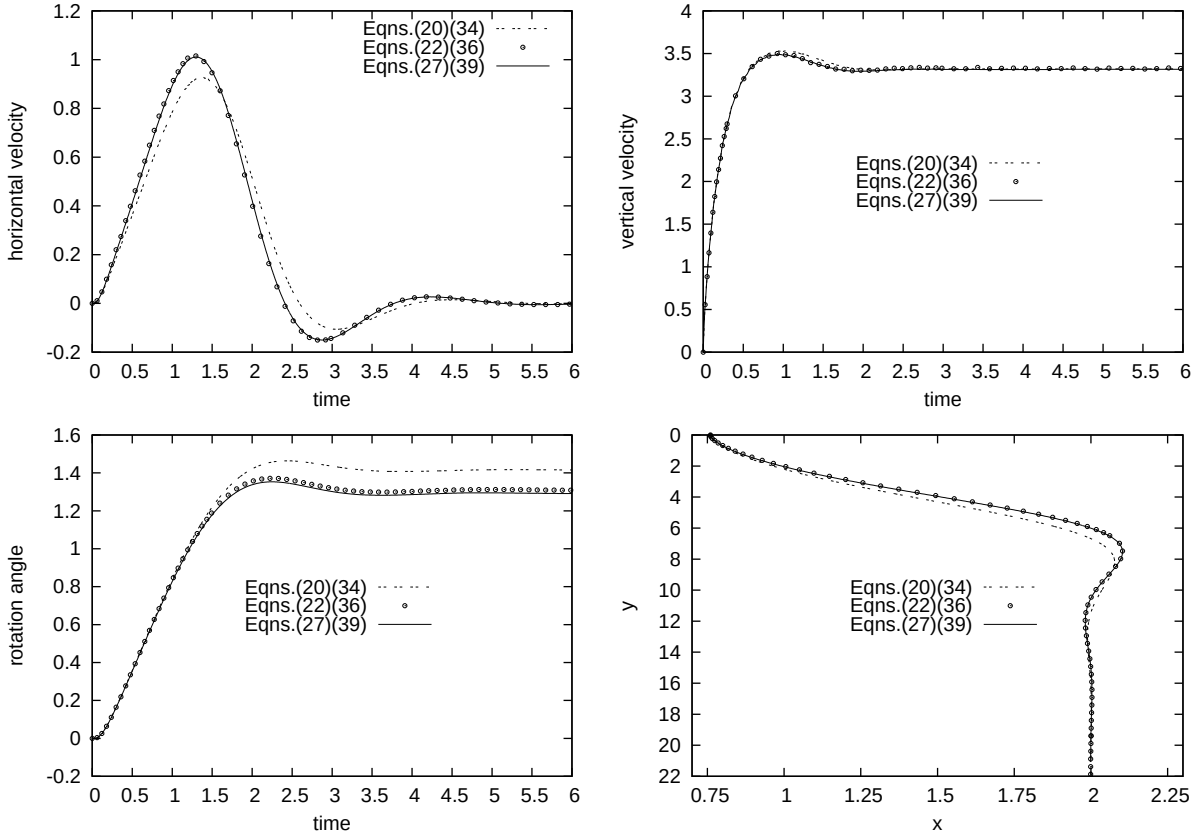

FIG. 6: Results obtained for the sedimenting disc of Figure 4 for $r_\rho = 1.01$. Time is expressed in seconds, space in millimeters, velocities in millimeters per second and angle in radians.

V. CONCLUSION AND DISCUSSION

In this work we have reviewed the momentum exchange method to compute the flow force and torque acting on a submerged body by presenting a new derivation. The

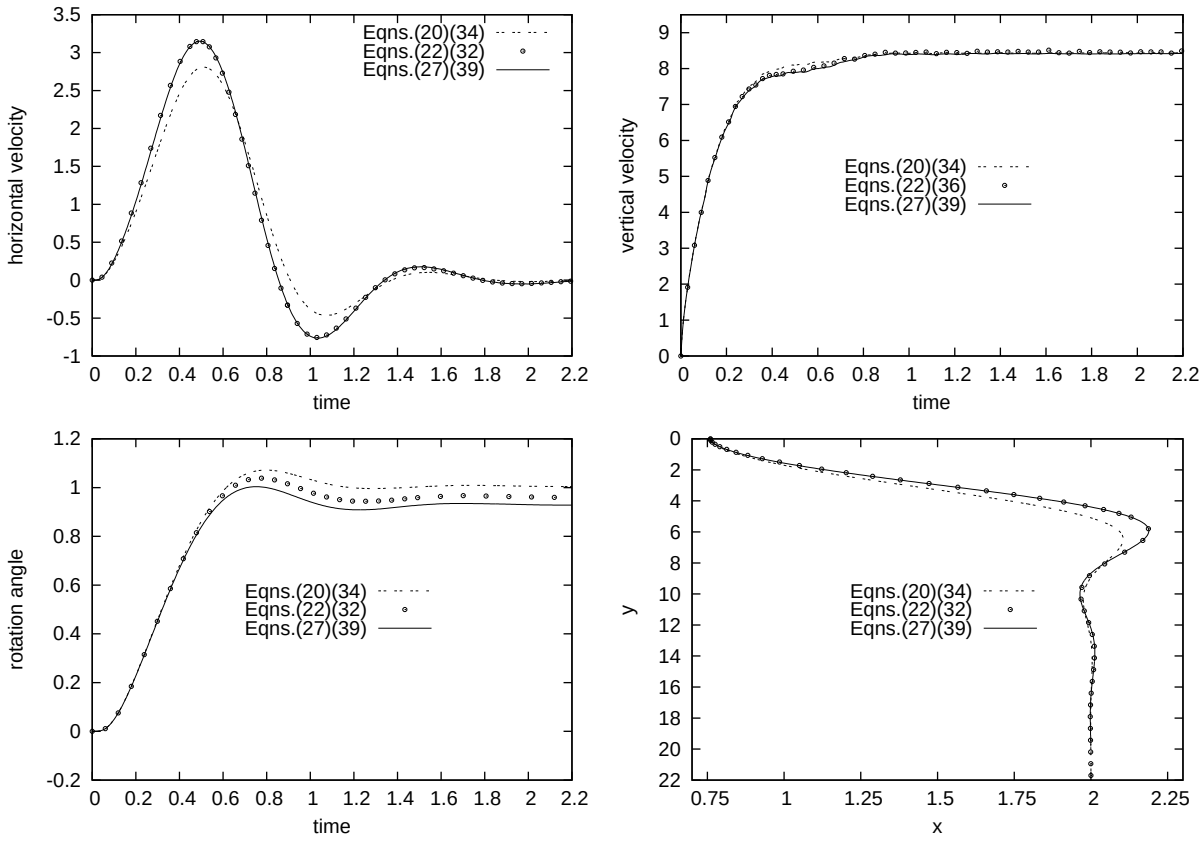

FIG. 7: Results obtained for the sedimenting disc of Figure 4 for $r_\rho = 1.03$. Time is expressed in seconds, space in millimeters, velocities in millimeters per second and angle in radians.

expressions we obtain, for the case of static bodies, are coincident with those presented in [9]. From our derivation we see that the expressions derived for the flow force and torque on static bodies are not appropriate to treat moving bodies. Moreover, we derive two of the proposals appearing in the literature to compute flow force and torque on moving bodies as particular cases. These last two alternatives to compute the force and torque are correct but different approximations to the same problem. The one consisting in (27) and (39) results in less noisy force and torque computations and is also more efficient from the computational point of view.

Our method of deriving momentum exchange does not use a particular treatment of the boundary conditions on the body surface and can be applied with several of the various methods proposed in the literature.

In the last part of the paper we have tested the corrected momentum exchange expressions we obtained by simulating two problems which are well know in the literature, a sedimenting circular disc and a sedimenting elliptic. Our results clearly show the difference, for the case of moving bodies, between the results of the corrected momentum exchange methods as compared to those given by equations (20) and (34). These results are in good agreement with those obtained by other authors using similar and different computational fluid dynamic methods such as finite element methods.

Acknowledgments

We want to thank Carlos Sacco and Ezequiel Malamud for useful discussions. J. P. Giovacchini is a fellowship holder of CONICET (Argentina). This work was supported in part by grants 05-B454 of SECyT, UNC and PIDDEF 35-12 (Ministry of Defense, Argentina). We want to thank the corrections and suggestions made by the referees that helped us improve our work.

[1] C. K. Aidun and J. R. Clausen, Annual Review of Fluid Mechanics **42**, 439 (2010).

[2] T. Inamuro, K. Maeba, and F. Ogino, International Jour-

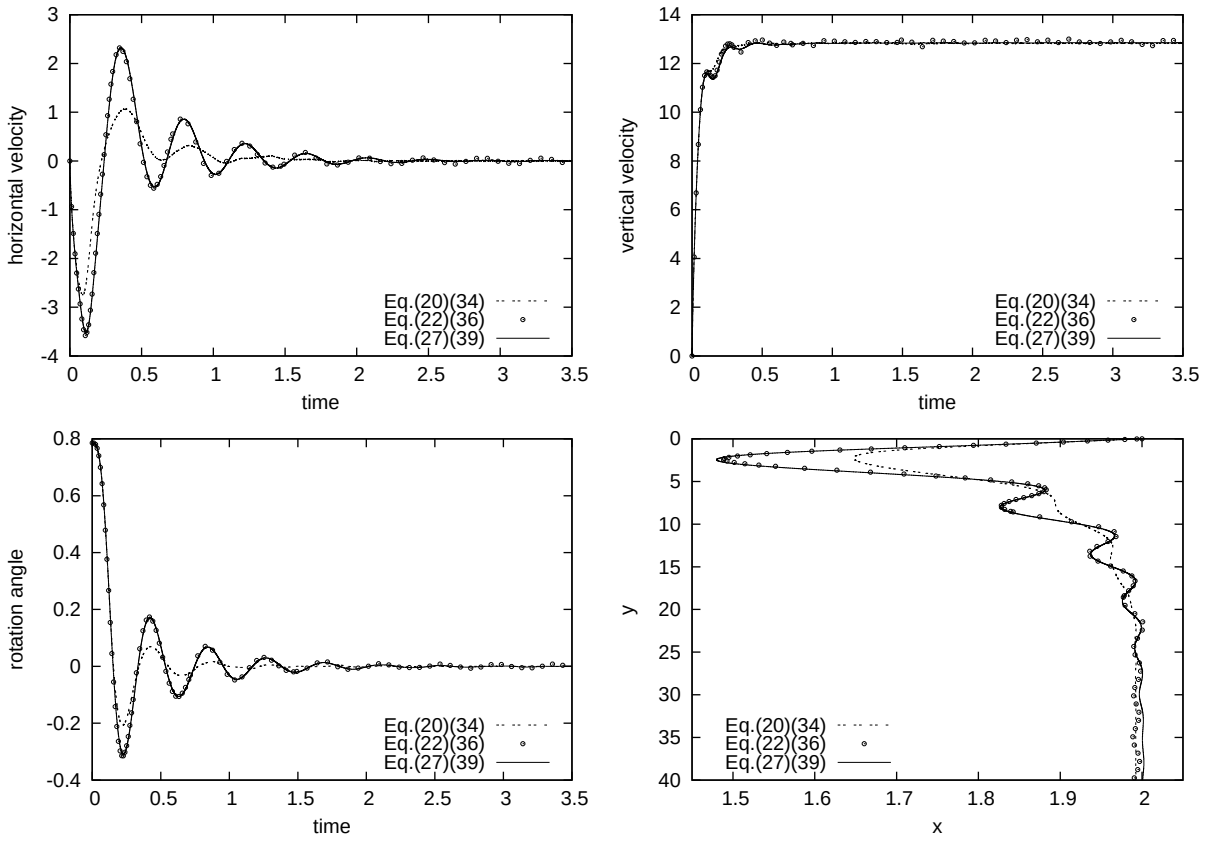

FIG. 8: Results for the sedimenting elliptical disc of Figure 5 using $r_\rho = 1.10$. Time is expressed in seconds, space in millimeters, velocities in millimeters per second and angle in radians.

nal of Multiphase Flow **26**, 1981 (2000), ISSN 0301-9322.

[3] Z. Xia, K. W. Connington, S. Rapaka, P. Yue, J. J. Feng, and S. Chen, Journal of Fluid Mechanics **625**, 249 (2009), ISSN 1469-7645.

[4] H. Li, X. Lu, H. Fang, and Y. Qian, Phys. Rev. E **70**, 026701 (2004).

[5] A. J. C. Ladd, Journal of Fluid Mechanics **271**, 285 (1994), ISSN 1469-7645.

[6] A. J. C. Ladd, Journal of Fluid Mechanics **271**, 311 (1994), ISSN 1469-7645.

[7] C. Aidun and Y. Lu, Journal of Statistical Physics **81**, 49 (1995), ISSN 0022-4715, URL `http://dx.doi.org/10.1007/BF02179967`.

[8] C. K. Aidun, Y. Lu, and E.-J. Ding, Journal of Fluid Mechanics **373**, 287 (1998), ISSN 1469-7645.

[9] R. Mei, D. Yu, W. Shyy, and L.-S. Luo, Phys. Rev. E **65**, 041203 (2002).

[10] P. Lallemand and L.-S. Luo, Journal of Computational Physics **184**, 406 (2003), ISSN 0021-9991.

[11] B. Wen, H. Li, C. Zhang, and H. Fang, Phys. Rev. E **85**, 016704 (2012).

[12] B. Wen, C. Zhang, Y. Tu, C. Wang, and H. Fang, J. Comput. Phys. **266**, 161 (2014), ISSN 0021-9991.

[13] S. Harris, *An Introduction to the Theory of the Boltzmann Equation*, Dover books on physics (Dover Publications, 2004), ISBN 9780486438313.

[14] Y. Sone, *Molecular Gas Dynamics: Theory, Techniques, and Applications*, Modeling and Simulation in Science, Engineering and Technology (Springer London, Limited, 2007), ISBN 9780817645731.

[15] X. He and L.-S. Luo, Phys. Rev. E **56**, 6811 (1997).

[16] S. Succi, *The lattice Boltzmann equation for fluid dynamics and beyond*, Numerical Mathematics and Scientific Computation (Oxford University Press, Oxford, 2001).

[17] D. Wolf-Gladrow, *Lattice-Gas Cellular Automata and Lattice Boltzmann Models: An Introduction*, no. n.° 1725 in Lattice-gas Cellular Automata and Lattice Boltzmann Models: An Introduction (Springer, 2000), ISBN 9783540669739.

[18] X. He and L.-S. Luo, J. Stat. Phys. **88**, 927 (1997).

[19] P. L. Bhatnagar, E. P. Gross, and M. Krook, Phys. Rev. **94**, 511 (1954).

[20] X. He and L.-S. Luo, Journal of Statistical Physics **88**, 927 (1997), ISSN 0022-4715.

[21] O. Filippova and D. Hnel, Journal of Computational Physics **147**, 219 (1998), ISSN 0021-9991.

[22] R. Mei, L.-S. Luo, and W. Shyy, Journal of Computational Physics **155**, 307 (1999), ISSN 0021-9991.

[23] R. Mei, W. Shyy, D. Yu, and L.-S. Luo, Journal of Computational Physics **161**, 680 (2000), ISSN 0021-9991.

[24] E.-J. Ding and C. Aidun, Journal of Statistical Physics **112**, 685 (2003), ISSN 0022-4715, URL `http://dx.doi.org/10.1023/A%3A1023880126272`.

[25] S. Krithivasan, S. Wahal, and S. Ansumali, Phys. Rev. E **89**, 033313 (2014).

[26] A. Caiazzo and M. Junk, Computers and Mathematics

with Applications **55**, 1415 (2008).
[27] J. R. Clausen and C. K. Aidun (????).
[28] J. Feng, H. H. Hu, and D. D. Joseph, Journal of Fluid Mechanics **261**, 95 (1994), ISSN 1469-7645.
[29] Q. Zou and X. He, Phys. Fluids E **9**, 1591 (1997).
[30] In incompressible-flow models, the same relation between δx and δt holds, but the constant c is no longer related to the speed of sound.
[31] The first method proposed to impose boundary conditions in LBM is known as bounce-back. Bounce-back was appropriate to treat rectilinear boundaries which are aligned with the lattice. The application of bounce-back when the boundary is of general shape would be equivalent to approximate the boundary of the body by a stair-step shape boundary coincident with lattice links, which implies a loose of accuracy.